Rapid communication

Uniform target ablation in pulsed-laser deposition

N. Arnold, D. Bäuerle

Angewandte Physik, Johannes-Kepler-Universität Linz, A-4040 Linz, Austria

Abstract. Pulsed-laser deposition (PLD) of uniform films with low particulate densities requires uniform target ablation. Optimal conditions are achieved when the target is rotated and simultaneously translated. The rotation, translation, and laser-pulse repetition frequencies must all be incommensurate. The target must be moved symmetrically to the fixed laser beam. The temporal dependence of the distance between the beam and the target center must follow the law $x_0 \propto t^{1/2}$. The best results are expected for a circular top-hat beam shape.

PACS: 81.15.Fg; 61.80.Ba; 42.62.Cf

Pulsed-laser deposition (PLD) has become a very popular technique for the fabrication of thin films of multicomponent materials [1]. Among the various materials investigated in detail are high-temperature superconductors, compound semiconductors, diamond-like carbon (DLC), dielectric, ferroelectric, and magnetic materials, various types of heterostructures, and organic polymers [1–4]. PLD is very reliable, offers great experimental versatility, is fairly simple, and is fast – as long as small-area films of up to several cm^2 are to be fabricated. For these reasons, PLD is particularly suitable in materials research and development. The strong nonequilibrium conditions in PLD allow some *unique* applications. Among these are *metastable* materials that cannot be synthesized by standard techniques, and the fabrication of films from species that are generated only during pulsed-laser ablation. With certain systems, the physical properties of such films are superior to those fabricated by standard evaporation, electron-beam evaporation, etc.

Besides restrictions with respect to film areas, the major disadvantages of PLD are related to particulates on the substrate and film surface and to inhomogeneities in the film thickness. These problems arise, in part, from surface roughening and structure formation on the target surface. With the development of surface structures, e.g. columnar features which align with the beam, the ablation rate decreases and the number of particulates increases with the number of laser

pulses [1, 5]. Additionally, with an uneven surface, the direction of plume expansion will continuously change, resulting in nonuniform material deposition. It has been demonstrated experimentally that these problems can be suppressed or even avoided if the target is simultaneously rotated *and* translated during ablation, as shown in Fig. 1 [1, 5, 6].

In this paper we study the problem of uniform target ablation theoretically, i.e. we determine the relative motion between the target and the laser beam that provides *uniform* ablation of the target.
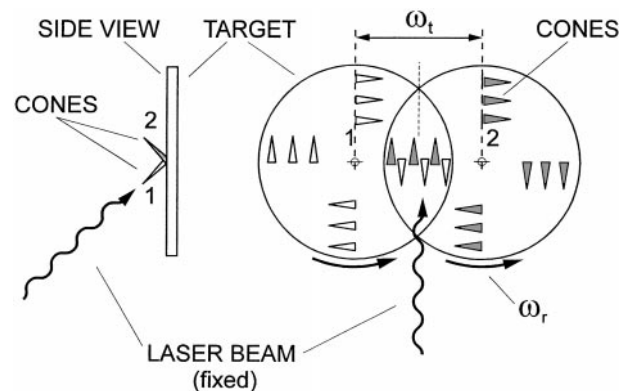
Fig. 1. Surface structures which align with the incident laser beam, e.g. columnar structures (cones), can be suppressed by simultaneous rotation and translation of the substrate with frequencies ω_r and ω_t, respectively. If the translation is symmetric with respect to the incident laser beam, each target site is ablated from opposing incident angles

1 Model

Let us first ignore the nonlinear dependence of the ablation rate on laser fluence. In this case, uniform ablation of the target is achieved if the (average) exposure provided by the laser beam is the same for all target points. In the laboratory system, the translation of the target is described by the vector $R(t)$ which is a periodic function of frequency ω_t (Fig. 2). The position of the laser beam with repetition frequency ω_l and
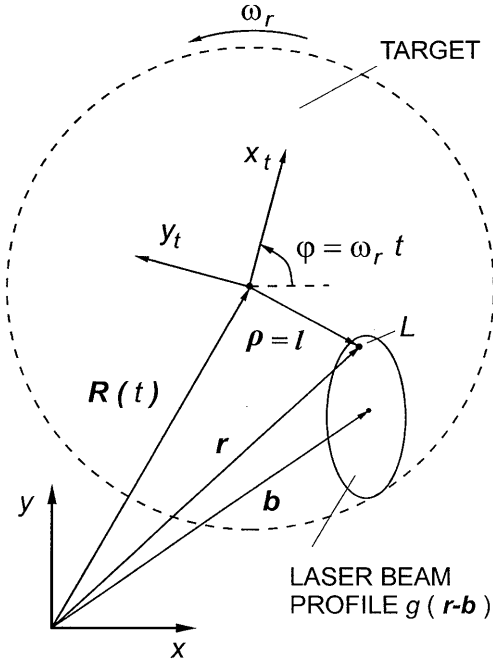
Fig. 2. Schematic picture of the reference frame (x_t, y_t) that rotates with the target with angular frequency ω_r. The movement of the target center is described by $\boldsymbol{R}(t)$, which is periodic with angular frequency ω_t. In the laboratory system (x, y) the center of the laser beam is positioned at a point $\boldsymbol{b}$. L is an arbitrary point within the laser beam with spatial profile g. The vectors from the center of the target to L in the laboratory system and the rotating systems are $\boldsymbol{\rho}$ and $\boldsymbol{l}$

spatial profile $g(\boldsymbol{r}-\boldsymbol{b})$ is described by the vector $\boldsymbol{b}$. The function g is, e.g., Gaussian, rectangular top-hat, etc. [1]. Consider an arbitrary point L on the target. In the reference frame *fixed with the target*, its position is given by $\boldsymbol{l} = (l_{x_t}, l_{y_t})$. The position of the point L *in the laboratory system* is $\boldsymbol{r} = \boldsymbol{R} + \boldsymbol{\rho}$ with

$$\boldsymbol{\rho} \equiv \begin{pmatrix} \rho_x \\ \rho_y \end{pmatrix} = \begin{pmatrix} \cos\omega_r t & -\sin\omega_r t \\ \sin\omega_r t & \cos\omega_r t \end{pmatrix} \begin{pmatrix} l_{x_t} \\ l_{y_t} \end{pmatrix} \equiv \hat{M}_\varphi \boldsymbol{l}, \qquad (1)$$

where $\hat{M}_\varphi$ is the rotation matrix with $\varphi = \omega_r t$. ω_r is the angular frequency of target rotation. The laser-beam intensity in L is

$$I(L) = jg(\boldsymbol{r}-\boldsymbol{b}) \equiv jg(\boldsymbol{R} + \hat{M}_\varphi \boldsymbol{l} - \boldsymbol{b}), \qquad (2)$$

where $j \equiv j(t)$ describes the temporal behavior of the intensity within the beam center. The *average* exposure in L is given by the temporal average of (2). This is calculated by Fourier expansion. The periodic function j is expanded into a Fourier series with terms $j_{n_1} \exp(i\omega_l n_1 t)$ where n_1 is an integer. The function g is first expanded into a Taylor series; the periodic functions $\boldsymbol{R}$ and $\hat{M}_\varphi \boldsymbol{l}$ in each Taylor term are then expanded into Fourier series with terms $\exp(i\omega_t n_2 t)$ and $\exp(i\omega_r n_3 t)$, respectively. As a result, the product jg in (2) will contain terms like $\exp[i(\omega_l n_1 + \omega_t n_2 + \omega_r n_3)t]$. If the frequencies ω_l, ω_t, and ω_r are incommensurate, all terms with $n_1 \neq 0$ will disappear upon averaging. Only terms with $n_1 = 0$ will remain. The common factor in this sum, $j_0 \equiv \langle j \rangle$, is the average intensity. Because $\langle j \rangle$ is a constant, the average of (2) can be written as

$$\langle I(L) \rangle = \langle j \rangle \langle g(\boldsymbol{R} + \hat{M}_\varphi \boldsymbol{l} - \boldsymbol{b}) \rangle. \qquad (3)$$

The average of $\langle g \rangle$ cannot be expressed in terms of $\langle R \rangle$, $\langle \hat{M}_\varphi \boldsymbol{l} \rangle$ and $\boldsymbol{b}$, as g is a *nonlinear* function of its argument. Equation (3) is a formal solution of the problem for arbitrary beam profiles g and target movements, $\boldsymbol{R}$. It is independent of the angular position on the target.

However, it is impossible to make the average exposure *strictly* independent of $\boldsymbol{l}$ for any simple function $\boldsymbol{R}(t)$. Nevertheless, we can find an approximate solution which yields an *almost* constant average exposure at each target site. This solution will now be derived.

Henceforth, it is more convenient to consider the center of the target as fixed, and the laser beam as scanned with frequency ω_t. Let us now choose a coordinate system that has its origin in the target center and which does *not* rotate with the target. Because the result of (3) will be the same for all $j(t)$ which yield the same $\langle j \rangle$, it is convenient to treat even pulsed-laser irradiation as cw with a constant intensity $\langle j \rangle$ in the beam center. A beam of finite size can be considered as a superposition of infinitesimally small beam elements with areas dS (Fig. 3). The average power in dS is $\langle j \rangle g\, dS$. dS moves with velocity $\dot{\boldsymbol{\rho}}$ with respect to the target center and it will cross the ring between ρ and $\rho + d\rho$ within the time

$$dt = d\rho/\dot{\rho}, \qquad (4)$$

where $\dot{\rho}$ is the radial component of $\dot{\boldsymbol{\rho}}$. During the time dt, the average exposure (energy per area) within the ring $2\pi\rho\, d\rho$ is

$$\langle d\phi(\rho) \rangle = \frac{\langle j \rangle g\, dS\, dt}{2\pi\rho\, d\rho} = \frac{\langle j \rangle g\, dS}{2\pi\rho\dot{\rho}}. \qquad (5)$$
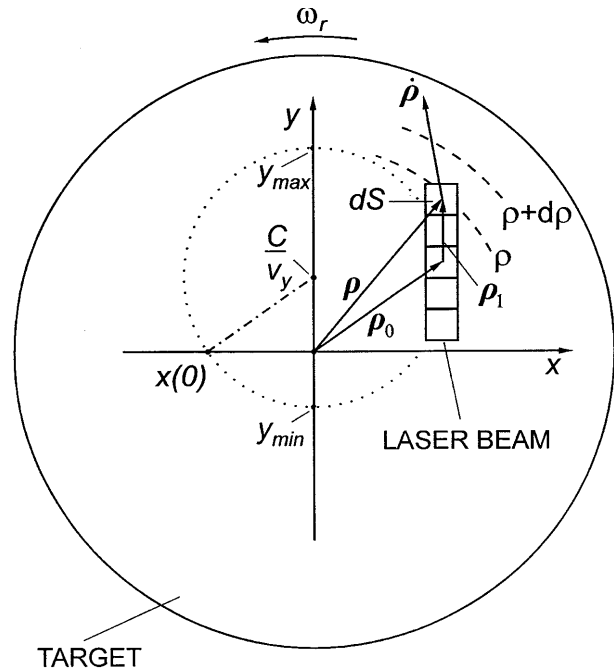
Fig. 3. Schematic picture of the movement of a vertical laser beam that provides uniform exposure. The origin of the (nonrotating) laboratory system is in the target center. An infinitesimal element of the beam, dS, moves with velocity $\dot{\boldsymbol{\rho}}$ and crosses the ring between ρ and $\rho + d\rho$ (*dashed*) with radial velocity $\dot{\rho}$. The vector $\boldsymbol{\rho}_1$ is directed from the beam center $\boldsymbol{\rho}_0$ to dS. The *dotted circle* shows the movement of the beam center which provides uniform exposure

Thus, if the product $\rho\dot\rho$ does not depend on ρ, i.e., if ρ and $\dot\rho$ obey the condition

$$\rho\dot\rho \equiv x\dot x + y\dot y \equiv \rho \quad \dot\rho = C = \text{const}(\rho)\,, \tag{6}$$

the exposure of the target by the beam element dS is uniform. For a finite beam size, (5) must be integrated over dS and the result becomes quite complicated, as in the general case the product $\rho\dot\rho$ and its dependence on ρ is different for each beam element. Nevertheless, if (6) is satisfied for each beam element (the values of C may differ for different elements), exposure will be uniform. It turns out that a movement of the *beam center* $\rho_0(t)$ for which *all* beam elements satisfy (6) does *not* exist. In order to verify this, we first consider a narrow, vertical beam with elements dS located at (see Fig. 3)

$$\rho(t) = \rho_0(t) + \rho_1\,, \tag{7a}$$

where ρ_1 is independent of time. In coordinates this can be written as

$$(x, y) = (x_0(t), y_0(t) + y_1)\,. \tag{7b}$$

The condition (6) can then be described by

$$x_0\dot x_0 + y_0\dot y_0 = C\,, \tag{8a}$$
$$x_0\dot x_0 + (y_0 + y_1)\dot y_0 = C_1 \Rightarrow y_1\dot y_0 = C_1 - C\,. \tag{8b}$$

If we choose $y_0 = 0$ for $t = 0$ we find

$$y_0 = \frac{C_1 - C}{y_1}t\,. \tag{9}$$

Equation (9) should hold for all beam elements with different y_1 and C_1. This requires

$$\frac{C_1 - C}{y_1} = v_y = \text{const} \tag{10}$$

and thus $y_0 = v_y t$. Integrating (8a) and substituting t for y_0 via (9) we obtain

$$x_0^2 + y_0^2 = 2Ct + x_0^2(0) \Rightarrow x_0^2 + \left(y_0 - \frac{C}{v_y}\right)^2 = x_0^2(0) + \frac{C^2}{v_y^2}\,. \tag{11}$$

This is the equation of a circle, which is shown in Fig. 3 by the dotted line. Thus, each element of the narrow vertical beam with its center ρ_0 moving along the circle centered on the y axis, will provide uniform exposure if the movement is such that the vertical velocity $|v_y|$ is constant [see (10)]. This results in the following statements.

1. If the beam has a *finite* width in the x direction, it is impossible to satisfy (6) for all beam elements, as the elements lying on the x axis would require rotation around a center located on the x axis and $v_x = \text{const}$, which is incompatible with $v_y = \text{const}$.
2. Different beam elements will cover different circular areas on the target. For example, the central beam element in Fig. 3, exposes only the region $|y_{\min}| \le \rho \le y_{\max}$. Thus, uniform exposure is achieved only in places where all these circular areas overlap.

Although one can further consider the movement based on the rotation described by (10) and (11), we concentrate on the particular case where the center of rotation tends to infinity, i.e. $C/v_y \to \infty$. In this case, the rotation degenerates into a vibration along the x axis. All further equations follow directly from (8).

$$\dot y_0 \equiv 0\,, \quad C_1 - C = 0\,, \quad \text{and} \quad x_0 = \sqrt{2C(t - t_0)}\,, \tag{12}$$

where t_0 describes an arbitrary initial time. Thus, a narrow (vertical) beam with arbitrary intensity distribution along ρ_1, vibrating in perpendicular direction according to (12), will provide a homogeneous exposure of the target.

2 Results and discussion

With oblique incidence of the laser beam, the target must vibrate *symmetrically* to the beam center, i.e., in the positive and negative x direction (Fig. 1). Only by this means, can the formation of columnar structures be suppressed. For this reason, we search for periodic motion with period $T_t \equiv 2\pi/\omega_t$ in the x direction. Such motion satisfing (12) can be described by

$$x_0 = \sqrt 2 R_t \left(\left|\frac{2t}{T_t} - \left[\frac{2t}{T_t}\right]\right|\right)^{1/2} \text{sign}\left(\frac{t}{T_t} - \left[\frac{t}{T_t}\right]\right)\,. \tag{13}$$

The square brackets indicate that the round value, i.e., the integer closest to a given value, should be taken. R_t is the amplitude of target oscillations in the x direction. With beam sizes $w_{x,y} \ll R_t$, the amplitude R_t is about equal to the radius of the target. The function (13) is shown in Fig. 4.

Subsequently, we shall discuss numerical simulations which illustrate the analytical results. Here, we assume a laser beam of *finite* size. The laser beam intensity incident on L is calculated from (2). The frequencies satisfy the condition $\omega_l : \omega_r : \omega_t = 10e : \pi : 1$. The exact values of the frequencies are unimportant as long as they are incommensurate.

Figure 5 shows the average exposure as a function of the normalized distance from the target center, ρ/R_t, for the four different beam shapes indicated in Fig. 6. The *full curve* corresponds to a top-hat circular beam that is symmetrically translated along the target diameter according to (13). Despite the finite beam size, exposure is quite uniform, apart
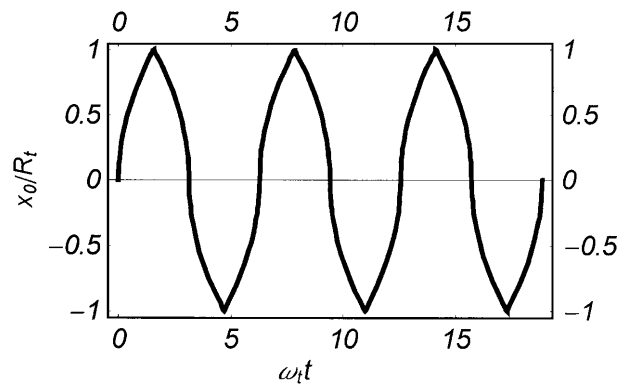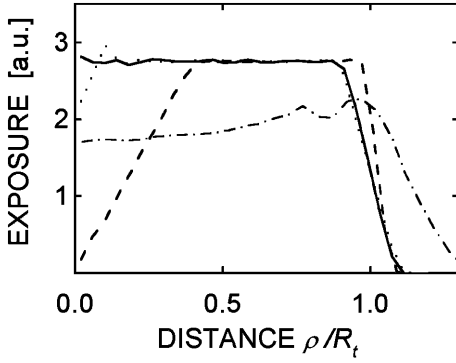

Fig. 4. Vibration of the beam center in the x direction as described by (13). For generality, dimensionless coordinates are chosen

Fig. 5. Dependence of the (average) target exposure on the (dimensionless) distance from the target center, ρ/R_t, calculated from (2) and (13). In all cases, the ratio of frequencies is $\omega_l : \omega_r : \omega_t = 10e : \pi : 1$. The different beam shapes employed have the *same* total power. $2w_x$ and $2w_y$ is the size of the beam in the x and y directions, respectively. *Solid curve*: top-hat circular beam with $w_x = w_y = 0.1R_t$; beam center at $\boldsymbol{b} = (0, 0)$. *Dotted curve*: top-hat square beam with $w_x = 0.1R_t$, $w_y = 0.1R_t$, $\boldsymbol{b} = (0, 0)$. *Dashed curve*: thin vertical top-hat rectangular beam with $w_x = 0.01R_t$, $w_y = 0.2R_t$, $\boldsymbol{b} = (0, 0.2R_t)$. *Dash-dotted curve*: top-hat rectangular beam with $w_x = 0.1R_t$, $w_y = 0.4R_t$, $\boldsymbol{b} = (0, 0.4R_t)$; sinusoidal translational motion

from edge effects. The good uniformity is also revealed from Fig. 6. The small wiggles outside the center are statistical. The slight elevation near the center is due to peripheral beam elements that are "too slow" when they cross the target center, as only the central part of the beam has the real square-root behavior (13); this results in an increase in laser-beam dwell time and correspondingly in a slight increase in average exposure. A Gaussian beam of the same size results in almost the same exposure, except that it is slightly less sharp near the target edge $\rho = R_t$. A twofold increase in beam size further decreases the slope near R_t. The final result depends on the exact size *and* shape of the beam. For example, a top-hat square beam (*dotted curve*) of the *same* size produces
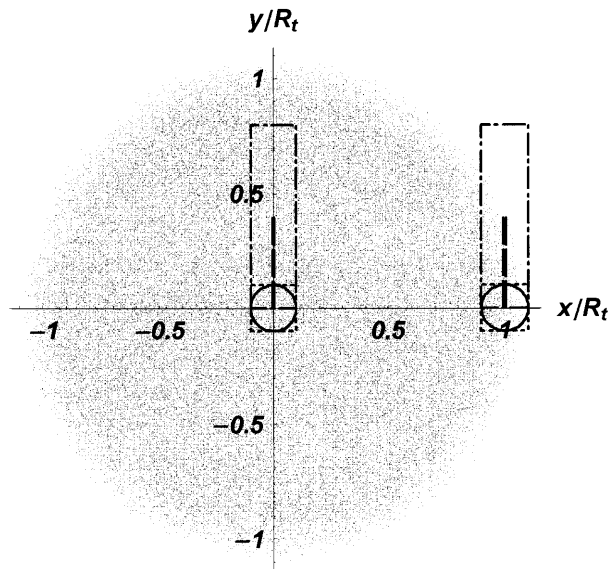
a significant *decrease* in exposure in the target center and overexposure at a distance w_x.

The *dashed curve* corresponds to a line-type vertical rectangular top-hat beam with the center shifted by w_y along the y axis. Such a beam provides uniform exposure within the region $2w_y < \rho < R_t$. With $\rho < 2w_y$ a linear decrease in intensity is observed. Similar behavior is obtained, for example, for a top-hat elliptical beam of the same area as the top-hat circular beam. For $w_y = 0.2R_t$, $w_x = 0.05R_t$ this results in a three-times lower average exposure near the center. If the elliptical beam is oriented in the x direction with $w_x = 0.2R_t$ and $w_y = 0.05R_t$, significant overexposure near the center is observed. The *dash-dotted* curve corresponds to a vertical top-hat rectangular beam (see also Fig. 6). In this case, the translational motion was *sinusoidal* with the same period and amplitude as in (13). The beam center was shifted in the y direction by w_y. Experimentally, such an arrangement provides rather uniform ablation [5]. Figure 5 shows that exposure is indeed rather uniform in the central part of the target, but not near the edge. The uniformity in the central part is somewhat accidental for such a large beam. It results from the competition of two effects. On the one hand, the sinusoidal translation is "too slow" near the center, which results in overexposure. On the other hand, as with the vertical line-type beam (dashed curve), underexposure within the center takes place. With the particular parameters employed, the second effect is more pronounced. This results in the overall decrease in exposure towards the center. This is, however, not a general trend, but it depends strongly on the size and/or shape of the beam.

The influence of nonlinearities

Up to now, we have assumed that the ablation rate is directly proportional to the local laser-beam intensity. This would be a good approximation for (linear) photochemical ablation, but certainly not for photothermal ablation [1]. This fact, however, will not significantly change the results. Let us make the following assumptions:

1. The spatial profile and intensity of laser pulses remain constant.
2. The laser pulse length, τ_l, is of nanoseconds or shorter, so that the rotation of the target can be ignored during the pulse ($\omega_r R_t \tau_l \ll w_{x,y}$).

Then, the intensity profile g can be recalculated as an ablation rate profile g_a. For example, if we ignore both radial heat conduction and screening due to the vapor plume, the local temperature rise near the ablation threshold is proportional to the local laser-beam intensity [1]:

Fig. 6. The density of points shows the exposure achieved with a top-hat circular beam (compare full curve in Fig. 5). For convenience, the different beam shapes discussed within the text are shown near the target center ($x_0 = 0$) and at the position $x_0 = R_t$

$$T(\boldsymbol{r}, t) - T_0 = \frac{A\alpha g(\boldsymbol{r})}{c\rho} \int_0^t j(t - t_1) \exp(D\alpha^2 t_1)$$
$$\mathrm{erfc}(D\alpha^2 t_1)^{1/2} \, \mathrm{d}t_1 \,, \qquad (14)$$

where D is the thermal diffusivity, α the absorption coefficient, and $c\rho$ the heat capacity per unit volume. Here, constant material parameters have been assumed. The ablated depth per pulse based on purely thermal evaporation is, near

threshold,

$$h(\boldsymbol{r}) \equiv h_0 g_a(\boldsymbol{r}) = \nu_0 \int\limits_0^\infty \exp\left(-T_a/T(\boldsymbol{r}, t)\right) \mathrm{d}t \,. \tag{15}$$

Here, ν_0 is a pre-exponential factor and h_0 the ablated depth within the beam center [1]. Thus, g_a is a complicated, but well-defined, functional of g. For realistic, i.e. Gaussian, beam shapes, the exponentiation of g which enters T in (15) will result in an almost Gaussian function g_a with smaller size. Significantly above threshold, $T(\boldsymbol{r}, t)$ and g_a must be calculated for the 1D or 3D ablation problem [1]. If screening by the plume becomes important during the pulse, a relation between g and g_a still exists but is not readily determined.

Equations (10)–(13), which are most important for practical applications, were derived for beams that are much smaller than the target, at least in one direction. As the numerical simulations show, the results hold, for example, for beam radii $w_{x,y} \approx 0.1 R_t$ (see Figs. 5 and 6). For beams of this size or smaller, the exact shape of g and/or g_a is not crucial, apart from effects near the center and near the edge $\rho \approx R_t$. In other words, the nonlinear dependence of the ablation rate on intensity will not significantly change the results discussed above. More important are incubation effects in weakly absorbing substrates [1]. Incubation centers accumulate with the number of laser pulses, and thereby do *not* allow one to treat all pulses as identical. Another problem lies in the columnar structures and surface instabilities that result in surface morphology changes with subsequent laser pulses.

3 Conclusion

Uniform ablation requires simultaneous rotation and translation of the target. For optimal conditions the translational motion must be symmetric with respect to the position of the laser beam. The frequencies of rotation, translation and laser-pulse repetition must be incommensurate. For an infinitesimally small beam, the translational motion along the diameter of the target must have a square-root dependence on time. For beams of finite size, the best results are achieved for a circular top-hat beam shape. A nonlinear dependence of the ablation rate on laser fluence does not significantly influence the results.

References

1. D. Bäuerle: *Laser Processing and Chemistry* (Springer, Berlin, Heidelberg 1996)
2. K. Yamamoto, Y. Koga, S. Fujiwara, F. Kokai, R.B. Heimann: Appl. Phys. A **66**, 115 (1998)
3. R. Schwödiauer, S. Bauer-Gogonea, S. Bauer, J. Heitz, E. Arenholz, D. Bäuerle: Appl. Phys. Lett. **73**(20), 2941 (1998)
4. R. von Helmolt, J. Wecker, B. Holzapfel, L. Schultz, K. Samwer: Phys. Rev. Lett. **71**, 2331 (1993)
5. E. Stangl, S. Proyer: PhD Thesis (Linz 1995)
6. C. Doughty, A.T. Findikoglu, T. Venkatesan: Appl. Phys. Lett. **66**, 1276 (1995)